

SIGNAL CANCELLATION EFFECTS IN ADAPTIVE RADAR MOUNTAINTOP DATA-SET

M. O. Berin *A. M. Haimovich*

Center for Communications and Signal Processing Research
E.C.E. Department
New Jersey Institute of Technology
University Heights
Newark, NJ 07102

ABSTRACT

This paper studies signal cancellation effects in adaptive radar. Using examples from Mountaintop data, it is shown that signal cancellation occurs when the target of interest is included in the weight vector training. The signal cancellation is due to calibration errors (mismatch between the target signal and presumed steering vector). An eigenanalysis-based adaptive beamformer is shown to have greater robustness to signal cancellation effects than the Sample Matrix Inversion (SMI) method.

1. INTRODUCTION

To achieve clutter rejection, the adaptive radar needs to estimate the statistical properties of the clutter process. Specifically, an adaptive weight vector is derived from the covariance matrix of the interference/clutter/noise. Over sections of homogeneous clutter, the covariance matrix can be estimated from signals received from the corresponding intervals of range cells. Commonly, the range cell under observation is excluded from the data set, and the estimate is based on a, so called, *secondary* data set. The rationale for a signal free training set is that array errors may cause signal cancellation. This effect is particularly evident with processing using the Sample Matrix Inversion (SMI) method, [1] [2]. Due to array imperfections, the *presumed* steering vector used as the reference representing the signal does not equal the *true* target response. Thus, the component of the true vector different from the presumed vector is interpreted as an interference, and the array proceeds to cancel it. This effect is particularly pronounced when the training set has limited data support. In this case, the information provided by the target range cells has a larger impact on the covariance matrix. Using a larger data set, however, may cause problems due to non-homogeneous clutter effects. The other alternative, retraining the processor anew for each range cell under test such that the cell excluded from the training set, adds considerable computational complexity. Consequently, techniques which are less susceptible to signal cancellation effects are of interest. Two types of errors are considered in this paper: (1) pointing errors, (2) calibration errors manifested as amplitude and phase errors. Two main approaches were suggested by researchers to mitigate the signal cancellation effects: (1) modification

of the beamformer constraints to widen the desired signal protection region and lessen the effects of mismatches [3], and (2) modifications of the steering vector [4].

Recently, eigenanalysis-based beamformers were considered for adaptive radar [5, 6]. In particular, the *eigencanceler* has been formulated as a modification of the minimum variance beamformer. The eigencanceler is the minimum norm weight vector that meets the set of linear constraints and is orthogonal to the interference subspace. In this paper we show that the eigencanceler is more robust than the SMI method with respect to signal cancellation effects. Elsewhere, this technique has also been shown to have significantly faster convergence [6], thus making it an attractive alternative to the SMI.

Section 2 of this paper contains the signal model and the performance analysis. Numerical results, including analysis of Mountaintop data, are provided in section 3. Our conclusions are contained in section 4.

2. PERFORMANCE CALCULATIONS

Consider a spatial processor with a single interferer and a single target. The correlation matrix is given by

$$\hat{\mathbf{R}} = \sigma_d^2 \mathbf{s}_d \mathbf{s}_d^H + \sigma_i^2 \mathbf{s}_i \mathbf{s}_i^H + \sigma_n^2 / L I, \quad (1)$$

where σ_d^2 , σ_i^2 , σ_n^2 are the desired signal, interference and noise power, and \mathbf{s}_d and \mathbf{s}_i are the desired signal and the interference vector, respectively. L is the number of antenna elements. For the spatial processor the normalized presumed steering vector has the form:

$$\mathbf{s}_m = \sqrt{1/L} [1 \quad e^{j2\pi\psi_m} \quad \dots \quad e^{j2\pi(L-1)\psi_m}]^T, \quad (2)$$

where ψ_m is the normalized spatial frequency and it is related to the presumed target angle, θ_m , by $\psi_m = d \sin \theta_m / \lambda$, where λ is the wavelength of the transmitted signal and d is the distance between antennas. The normalized desired signal vector has the form

$$\mathbf{s}_d = \frac{1}{|\mathbf{c}|} [c_0 \quad c_1 e^{j2\pi\psi_d} \quad \dots \quad c_{L-1} e^{j2\pi(L-1)\psi_d}]^T, \quad (3)$$

and

$$\mathbf{c} = [c_0 \quad c_1 \quad \dots \quad c_{L-1}]^T, \quad (4)$$

where c is a complex random variable with Gaussian-distributed magnitude and phase. Assuming good calibration, both the magnitude and the phase have small variances. The vector \mathbf{c} models the calibration errors. The

⁰This work was supported by AFOSR-Rome Laboratories under grant F30602-94-1-0012

mean of the amplitude is $\sqrt{1/L}$ and the mean of the phase errors is zero. The difference between the true angle and presumed angle, $\theta_m - \theta_d$, is the pointing error. Under ideal conditions of no calibration and pointing errors, the desired signal vector equals the presumed steering vector. Since the interference signal goes through the same channels as the desired signal, the normalized interference vector is given by

$$\mathbf{s}_i = \frac{1}{|c|} \left[c_0 \quad c_1 e^{j2\pi\psi_i} \quad \dots \quad c_{L-1} e^{j2\pi(L-1)\psi_i} \right]^T, \quad (5)$$

where ψ_i is the normalized spatial frequency of the interference. To compare the performance of the adaptive beamformers, the array gain, defined as the ratio of the SNIR at the output of the beamformer to the SNR at the input of the beamformer, is used. The array gain, as a function of the weight vector, is given by

$$G(\mathbf{w}) = \frac{|\mathbf{w}^H \mathbf{s}_d|^2}{\text{INR} \mathbf{w}^H \mathbf{s}_i \mathbf{s}_i^H \mathbf{w} + 1/L \mathbf{w}^H \mathbf{w}}, \quad (6)$$

where $\text{INR} = \sigma_d^2 / \sigma_n^2$.

The SMI method uses the weight vector

$$\mathbf{w}_{smi} = k \hat{\mathbf{R}}^{-1} \mathbf{s}_m, \quad (7)$$

where $\hat{\mathbf{R}}$ is the estimated correlation matrix of the interference and k is a gain constant [7]. The vector \mathbf{w}_{smi} is the optimal solution for the likelihood ratio detector if components of the array vectors are distributed jointly Gaussian and the interference is a stationary process with known covariance matrix. In practice the correlation matrix is estimated using a finite window of data with no target present. In this case the solution is not optimal anymore. It has been shown that a data support of at least $2L$ is needed for the SMI to converge within 3 dB of the optimal solution [7]. This convergence rate is very slow and it might be even larger if the data is not homogeneous.

The eiganceller's weight vector is given by

$$\mathbf{w}_{eig} = k(\mathbf{I} - \mathbf{Q}_i \mathbf{Q}_i^H) \mathbf{s}_m, \quad (8)$$

where k is a gain constant, \mathbf{Q}_i is an $L \times r$ matrix whose columns are the interference subspace eigenvectors. For the correlation matrix given in equation (1) the rank of the interference subspace is one ($r = 1$). The eiganceller is a suboptimal beamformer with a weight vector constrained to the noise subspace [8].

The effects of array imperfections are studied by plotting the array gain in equation (6) as a function of the pointing error, the SNR and standard deviation of phase errors, for both the SMI and the eiganceller. Details of the analysis presented below can be found in [9]. For the spatial case when the interference vector is orthogonal to the true target, $\mathbf{s}_i^H \mathbf{s}_d = 0$, and only pointing errors are considered, ($c_i = \sqrt{1/L}$), then the array gain for the SMI is given by

$$G_{smi} = \frac{|\rho_1|^2 (1 - \gamma_s)^2}{1 - \gamma_s (2 - \gamma_s) |\rho_1|^2 - \gamma_i (2 - \gamma_i) |\rho_2|^2} \quad (9)$$

where $\rho_1 = \mathbf{s}_m^H \mathbf{s}_d$, $\rho_2 = \mathbf{s}_m^H \mathbf{s}_i$, $\gamma_s = \text{SNR} / (1 + \text{SNR})$, and $\gamma_i = \text{INR} / (1 + \text{INR})$. Note that $0 \leq \gamma_s, \gamma_i \leq 1$. As observed by other authors through similar analysis, G_{smi} degrades as SNR increases. In the extreme case, $\text{SNR} = \infty$ ($\gamma_s = 1$), and $G_{smi} = 0$. The other extreme is $G_{smi} = |\rho_1|^2 / (1 - |\rho_2|^2)$, obtained for $\gamma_s = 0$ and $\gamma_i = 1$. For the eigenanalysis-based technique it can be shown that:

$$G_{eig} = \frac{|\rho_1|^2}{1 - |\rho_2|^2} \quad (10)$$

From equations (9) and (10) it is observed that $G_{smi} \leq G_{eig}$, with the equality for $\gamma_s = 0$ and $\gamma_i = 1$. Consequently, the eigenanalysis method is less affected by pointing errors than the SMI method. Expressions for the array gain for the general case where the signal and interference vectors are not orthogonal, are more complicated and can be found in [9].

The signal cancellation effects of both methods are illustrated in figures below. In all figures the SNR axis measures the quantity $(\sigma_d^2 + \sigma_i^2) / \sigma_n^2$. Figure 1 is generated using equation (6) and it shows the effects of SNR and the pointing error on the array gain. There are no phase and amplitude errors, ($c_i = \sqrt{1/L}$). The target is at bore sight ($\theta_d = 0^\circ$), and the interference angle is -15° . When the SNR is small (0 dB in the figure corresponds to $\sigma_d^2 = 0$), pointing errors have the least effect on the array gain. As the SNR increases, the SMI's mainlobe narrows and the performance degrades for even a small pointing error. The eiganceller's performance is acceptable up to the SNR of approximately 15 dB, but it decreases as SNR values approach INR. This behavior is due to the shift of the first eigenvector towards the desired signal as the SNR approaches the INR. When the SNR is equal to the INR, the eiganceller fails even when there are no pointing errors, since the first eigenvector has a large projection on the desired signal, which causes signal cancellation.

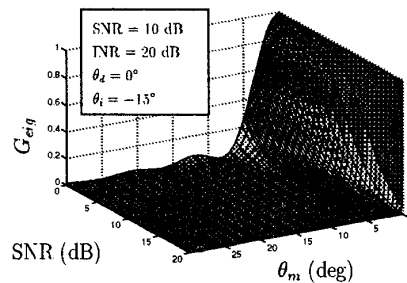
In Figure 2, effects of the phase and pointing errors are studied. There are no amplitude errors and the phase errors are modeled as a zero-mean Gaussian random variable. Phase errors were evaluated using 50 Monte Carlo runs. The SMI exhibits a larger degradation in the array gain than the eiganceller, as a function of both pointing and phase errors. It is observed that the SMI gain is decreased to 1/2 for phase errors with a standard deviation of 5° , while the eiganceller exhibits almost no loss of performance for phase errors up to 8° .

3. MOUNTAINTOP DATA ANALYSIS

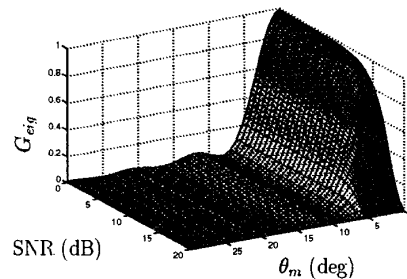
In this section, the performance of the eiganceller and SMI are compared using Mountaintop data. Two main assets of the Mountaintop Program are the Radar Surveillance Technology Experimental Radar (RSTER) and Inverse Display Phase Central Array (IDPCA). The system is described in [10]. RSTER is a 5 meter by 10 meter vertically polarized array made up of 14 row elements with an independent phase shifter, transmitter and receiver. For a fixed radar, IDPCA produces clutter returns with the same spatial and temporal characteristics as observed from an airborne surveillance platform. Analysis was carried out

on IDPCA data recorded on Feb 10, 1994 at North Oscura Peak, White Sands Missile Range (WSMR), New Mexico. For the data set referred to as t38pre01v1.mat, IDPCA was applied to emulate clutter at 245° and 156 Hz in Doppler. The synthetic target was injected at 154 km in range, 275° in angle, and 156 Hz in Doppler. The boresight angle was 260° . The pulse repetition frequency (PRF) was 625 Hz. Data was recorded from $865 \mu\text{s}$ to $1298 \mu\text{s}$ after the pulse was transmitted, corresponding to range cells from 130 km to 195 km with a range resolution of 150 m. Data was recorded in coherent pulse intervals (CPI) with 16 PRI's. The normalized Doppler frequency of both the target and the interference was 0.250.

The data analyzed was post-Doppler, i.e. following Doppler processing. For each range, a 16×14 matrix was formed, where the columns of this matrix contain temporal information and the rows contain spatial information. At each antenna, the received signals were processed using fixed Doppler filters. The Doppler filter containing the target and clutter was selected for follow-up processing. Thus spatial processing was applied to 14×1 data vectors. The spatial steering vector was formed using the known target angle. The data was plotted relative to sky noise. To calculate the sky noise level at the output of the beamformer, the weights calculated for a specific experiment were applied to the sky noise data. The mean of the sky noise output was used as reference for the plots generated. The performance of the SMI and eigencanceller methods are compared in Figure 3. The performance of the non adaptive array (application of a steering vector in the direction of the target) is also provided. Weight vectors were computed from a 50 data point training set. In part (a), the training range cells were from 145 km to 152 km (outside the target region). Both the SMI and the eigencanceller methods detect the target and suppress the clutter. The non-adaptive beamformer provides an indication where the clutter is present in range. An important observation is that the SMI method provides deep cancellation of the training region. This is due to the fact the covariance matrix is 'known' in this region. In part (b), the training is applied around the target region from 150 km to 158 km with the target region, 5 range cells, omitted from the training set. The eigencanceller's performance is almost unchanged. The performance of the SMI is decreased by 4 dB, due to residual cancellation effects to which the SMI method is sensitive. Omitting the target region is not a practical approach since the weight vector needs to be recalculated for each range cell under test. A more realistic approach is given in part (c), where all the data vectors were used for training, including the target region. The presence of the target region in the training set causes an increase in the desired signal component in the estimated correlation matrix. This, put together with calibration errors, causes a deep signal cancellation by the SMI method, as predicted in the analysis section. As expected, the eigencanceller is only slightly affected by the presence of the signal in the training set.



(a) Sample Matrix Inversion



(b) Eigencanceller

Figure 1. Effects of Signal-to-Noise Ratio and Pointing Error on Array Gain

4. CONCLUSIONS

We have shown, by analysis and illustrations from the Mountaintop dataset, that adaptive radar is susceptible to signal cancellation effects when the target signal is included in the training data and in the presence of pointing/calibration errors. It was shown that signal cancellation with the SMI method is very sensitive to the SNR and to the magnitude of the pointing/calibration errors. It was also shown that eigenanalysis-based adaptive radar is much more robust than the SMI with respect to signal cancellation effects.

REFERENCES

- [1] H. Cox, "Resolving power and sensitivity to mismatch of optimum array processors," *J. Acoustics Society of America*, vol. 54 No. 1, pp. 771-785, 1973.
- [2] N. K. Jablon, "Adaptive beamforming with the generalized sidelobe canceller in the presence of array imperfections," *IEEE Trans. Antennas and Propagation*, vol. 34 No. 8, pp. 996-1012, Aug. 1986.
- [3] M. H. Er and A. Cantoni, "An alternative formulation for an optimum beam-former with robustness capability," *Proc. Inst. Elec. Eng.*, pp. 447-460, Oct. 1985.
- [4] D. D. Feldman and L. J. Griffiths, "A projection approach for robust adaptive beamforming," *IEEE Trans. Signal Processing*, vol. 42 No. 4, pp. 867-876, Apr. 1994.
- [5] I. P. Kirsteins and D. W. Tufts, "Adaptive detection using low rank approximation to a data matrix," *IEEE Trans. Aerospace and Electronic Systems*, vol. 30, pp. 55-67, Jan. 1994.

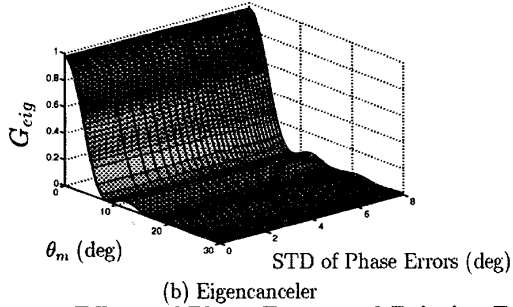
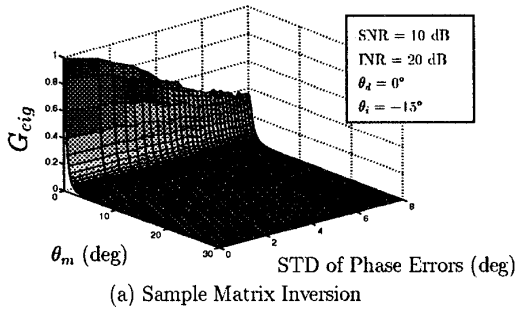


Figure 2. Effects of Phase Errors and Pointing Error on Array Gain

- [6] A. M. Haimovich, "The eigencanceler: Adaptive radar by eigenanalysis methods," *IEEE Trans. Aerospace and Electronic Systems*, 1996. to appear.
- [7] I. S. Reed, J. D. Mallett, and L. E. Brennan, "Rapid convergence rate in adaptive radar," *IEEE Trans. Aerospace and Electronic Systems*, vol. 10 No. 6, pp. 853-863, Nov. 1974.
- [8] A. M. Haimovich and Y. Bar-Ness, "An eigenanalysis interference canceler," *IEEE Trans. Signal Processing*, vol. 39 No. 1, pp. 76-84, Jan. 1991.
- [9] M. O. Berin, "Analysis on calibration, robustness, detection of space-time adaptive radar using experimental data," Master's thesis, New Jersey Institute of Technology, Jan. 1996.
- [10] G. W. Titi, "An overview of the ARPA mountaintop program," in *Proceedings of Adaptive Antenna Systems Symposium*, Long Island, NY, pp. 53-59, Nov. 1994.

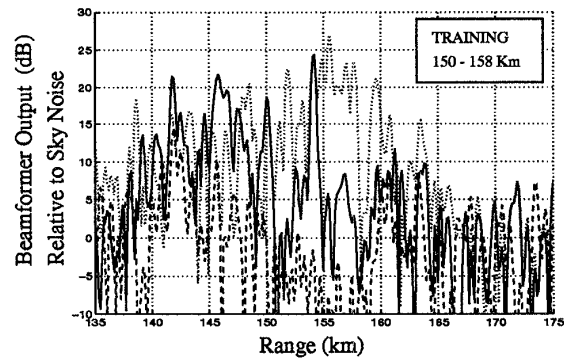
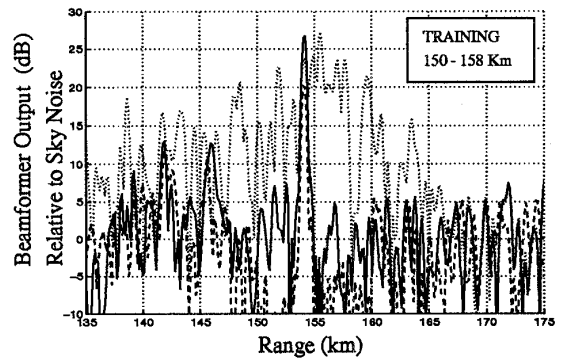
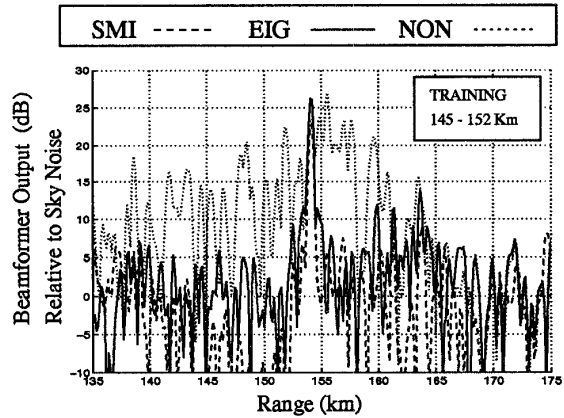


Figure 3. Post-Doppler Range Plots Using 50 Training Points